ISSN 1648-4142 / eISSN 1648-3480

VILNIUS TECH
Vilnius Gediminas Technical University

TRANSPORT

2023
Volume 38
Issue 3
Pages 127–138
https://doi.org/10.3846/transport.2023.19795

Original Article

EXPERIMENTAL STUDY ON DRIVER'S MENTAL LOAD IN HAIRPIN CURVES OF MOUNTAINOUS HIGHWAY

Ying CHEN[1]✉, Xiaohui WANG[2], Xiaobo ZHANG[2], Haiyuan CHEN[3], Zhigang DU[1], Jin XU[3,4]

[1]*School of Transportation and Logistics Engineering, Wuhan University of Technology, Wuhan, China*
[2]*China Railway Siyuan Survey and Design Group Co., Ltd., Wuhan, China*
[3]*College of Traffic and Transportation, Chongqing Jiaotong University, Chongqing, China*
[4]*Chongqing Key Laboratory of "Human–Vehicle–Road" Cooperation and Safety for Mountain Complex Environment, Chongqing Jiaotong University, Chongqing, China*

Highlights:

- 1st study of driving mental load at mountain hairpin curves;
- entrance environment differences result variety in hairpin curve heart rate patterns;
- overall driver heart rate distribution ranges showed 2 trends;
- 4 patterns of heart rate variability (HRV) were classified.

Article History:

- submitted 23 October 2021;
- resubmitted 9 December 2022;
- accepted 23 February 2023.

Abstract. In order to reveal the driving psychological characteristics and influencing factors of drivers under the hairpin curve section, 11 continuous hairpin curves on mountain roads were selected for natural driving test, and the on-board instruments were used to collect the driver's ElectroCardioGraphy (ECG) under the natural driving habits. Analyse the overall heart rate characteristics, Heart Rate Increase (HRI), Heart Rate Variability (HRV) characteristics of drivers, as well as the relationship between heart rate change and the visual performance of curve corner and slop and curve environment. And compared with the general curve. The results show that: with 180° as the limit, the curve angle of the hairpin curve was divided into 3 types: greater, less or approximate. The 3 types of curve angle have different effects on the driver's heart rate fluctuations. The overall heart rate distribution can be divided into 2 regions, in which the average heart rate of each driver at the curve, which curve angle ≈ 180°, was higher than the other 2 types of curves. The overall fluctuation range of heart rate in the middle of the curve is at the lowest level in the 3-stage curve segment area. Through the eigenvalue analysis of HRI, it can be seen that the drivers were more susceptible to the external environment when going downhill. When going uphill, the distribution range of the heart rate abnormality value was stable, but the sudden change was obvious. However, during the downhill direction, the overall adjacent heart rate varies greatly, but the abrupt change was small. Take the change trend of the HRI in the curve segment as an indicator, heart rate types were divided into 4 categories, continuous tension, relax gradually, relaxation-tension, and tension-relaxation. The 4 modes have a significant relationship with the difference of curve entrance environment. Compared with the modes shown in general curves, they focus on the modes with greater volatility, while the general curves focus on a more single growth trend.

Keywords: traffic engineering, hairpin curve, mountain road, natural driving test, driving mental load, heart rate variability.

✉Corresponding author. E-mail: *yingchen1108@qq.com*

Notations

ECG – electrocardiography;
HRI – heart rate increase;
HRV – heart rate variability;
RMSSD – root mean square value.

Introduction

The hairpin curve is a commonly used alignment unit that conforms to the terrain in a complex topographic environment. The curve deflection angle is large, the curve length is short, the radius is small, and the roadside environment is complicated. The large centrifugal force during curve increases the driving risk factors and reduces the comfort.

There are high requirements for driving skills, and the driver is highly nervous when driving, which seriously affects driving safety. At this stage, most researches on driving behaviour in complex areas focus on driving speed and other research (Russo *et al.* 2016; Eboli *et al.* 2017), and heart rate is an intuitive reflection of the driver's mentality changes and tension. Because of the simple collection method, it is often used for driving load research. Through analysis, it is also easy to make safety improvement suggestions from the driver's perspective. The research on the driver's heart rate mainly focuses on the following aspects:

- the ***1st aspect*** is the driver's heart rate changes during bridge and tunnel driving. Comparative study on the heart rate changes in the transition section of the tunnel and the tunnel section was conducted (Miller, Boyle 2015). Driving simulator were used to study the driver's heart rate under different conditions, in order to detect the safety of the lowest point of urban river-crossing tunnels (Feng *et al.* 2017). The influencing factors of the driver's heart rate in the underpass tunnel were studied, and found that the gradient has a greater influence on the driver's heart rate than the speed. Heart rate changes when going downhill is higher than when going uphill (Feng *et al.* 2018). At the same time, research has analysed the influence of tunnel greening on the driver's heart rate (Xiao *et al.* 2017). And according to the HRV index to study the mental condition of the drivers in the extra-long highway tunnel (Qin *et al.* 2021);
- the ***2nd aspect*** is heart rate is correlated with road alignment parameters, environment, etc. The influence of the blue and white deceleration signs on the side of the road on the driver's heart rate and speed were studied (Wu *et al.* 2013). Also, driver's heart rate characteristics were analysed and discussed when driving at the spiral ram, and the heart rate values at the split and merge points were significantly higher than the rest of the spiral ramp (Xu *et al.* 2020). And then, the relationship between the radius of the curve and the heart rate has been analysed, and obtained a reasonable design value for the radius of the curve, $r \geq 900$ m and $200 \leq r \leq 300$ m (Zhang *et al.* 2015). As well as the relationship between the driver's heart rate and the road curve ratio on the construction road (Qiao *et al.* 2020). At the same time, some scholars conducted experiments on different grades of roads to analyse the differences in heart rate of drivers in different road environments (Zhao *et al.* 2016). And in order to strengthen the safety level of the 2-lane highway, the law of change between the horizontal curve radius of the 2-lane mountain highway and the driver's heart rate was analysed (Zhao, Zhang 2012);
- the ***3d aspect*** is fatigue driving research. 2 methods for detecting driver's fatigue driving were discussed, including the measurement of driver's heart rate and the method of driver behaviour (Wadhwa, Roy 2020). Bracelet was used to measure the driver's heart rate to detect fatigue driving (Wolkow *et al.* 2020). HRV was used as a physiological indicator of the human body and an artificial intelligence-based early detection system for driver fatigue was introduced (Patel *et al.* 2011). The ECG sensor was used to obtain the heart rate variation coefficient to detect driving fatigue (Gromer *et al.* 2019). And through the perception speed test of bus drivers in Beijing (China) to study driver fatigue (Sang, Li 2012). Through the calculation of HRV, the fatigue problems of drivers of different genders were analysed, and the relationship between HRV and the driver's autonomic nervous system was obtained (Zeng *et al.* 2020). The existing fatigue driving based on the heart rate criterion has been reviewed, which can help to understand the research system (Zhu 2020);
- the ***4th aspect*** is research on roads with special terrain, such as research on plateau roads, the effect of the angle of the horizontal curve on the physiological load of the driver by defining the heart rate growth rate and the pulse blood volume distribution coefficient (Wang, Alli 2020). And prairie highway research, by collecting data on the driving behaviour, reaction time and electrocardiogram results of drivers while driving on the prairie highway, study the driving fatigue of prairie highways (Peng *et al.* 2021). And for the study of the forest zone, analysed the psychological load of drivers on icy and snowy roads in forest areas and the calculation of heart rate growth rates resulted in greater heart rate indicators for drivers driving at high speeds on snow and ice roads (Li *et al.* 2015).

In summary, the research on heart rate mainly concentrated on grasslands, plateaus, icy and snowy areas, bridges and tunnels or general mountain roads. The line shape is a road with a larger curve angle and a larger radius value. There is no research on the driver's heart rate at the hairpin curve under the extreme conditions of road design. Therefore, in order to clarify the psychological characteristics and influencing factors of drivers when driving at the hairpin curve, the heart rate indicators collected in the actual vehicle test of the driver were used to evaluate the psychological load of the complex and high-risk driving environment at the hairpin curve in the mountainous area. The research results can provide a reasonable reference standard for driving safety, driving comfort and road warning signs and markings at the hairpin curve.

1. Methods

1.1. Test road

A low-grade road in Pengshui County, Chongqing (China) was selected as the test object, and the design speed of the road section (Class IV mountain road) is 20 km/h, the road surface is in good condition, and the road markings are clear. The experimental section has a total length of 8.7 km and contains multiple hairpin curves. According to the measured data and terrain conditions, the specific parameters are shown in Table 1. The test road is shown in Figure 1.

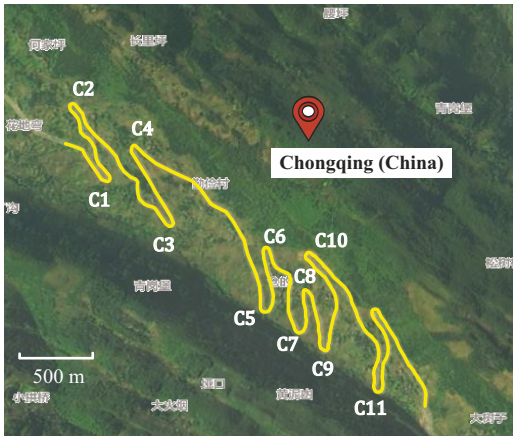

Figure 1. Test road

Figure 2. Test instruments:
(a) Prince 180D rapid electrocardiograph;
(b) SV-MDOO9HD driving recorder

Table 1. Geometric parameters of the hairpin curves

Number	Radius [m]	Curve angle [°]	Curve length [m]	Slope [%]	Lane width [m]	Road width [m]
1	20.156	192.73	92.975	3.0	4.25/4.25	10
2	20.233	186.19	90.797	3.0	4.25/4.25	10
3	20.079	180.09	88.138	3.0	4.25/4.25	10
4	20.029	169.51	84.381	3.0	4.25/4.25	10
5	20.425	159.43	87.519	2.7	4.25/4.25	10
6	20.861	190.62	94.561	2.8	4.25/4.25	10
7	22.315	150.60	83.815	3.0	4.75/3.55	10
8	20.260	172.64	86.202	3.0	4.25/4.25	10
9	20.304	186.58	91.257	3.0	4.25/4.25	10
10	20.327	180.54	89.188	3.0	4.25/4.25	10
11	20.347	194.54	94.259	3.0	4.25/4.25	10

1.2. Subjects and equipment

The trial recruited 20 drivers from the society, ranging in age from 22 to 48 years old, with an average age of 29.95 years. The driving age is 4...30 years, the average driving age is 11.93 years. The driving mileage is $1.8 \cdot 10^4$ km to $20 \cdot 10^4$ km, and the average mileage is $8.4 \cdot 10^4$ km. It was required that there was no emergency on the day of the test to reduce the influence of external factors on the heart rate value of the driving process.

The test vehicle is a small passenger car. The 7-seat commercial vehicle Buick GL8 is specifically selected with a large internal space, in order to facilitate the installation of test equipment and the test personnel to operate the data collection instrument on the car. In order to collect dynamic ECG signals, the Prince 180D rapid electrocardiograph was used to collect the heart rate (Figure 2) and use the on-board SV-MDOO9HD driving recorder to record the driving video of the vehicle for later data processing and verification.

1.3. Test conditions and requirements

In order to ensure the normal rhythm of the human body (the heart rate of a normal adult is 50 to 100 bpm, and the maximum is not more than 160 bpm), the test time was from 9:00 am to 5:00 pm during the day, and there was no severe weather such as heavy rain. After the driver gets in the car, the tester wears a heart rate monitor. The 3 ports were attached to the left and right chest and right lower abdomen. A new driver was created in the heart rate monitor. After the heart rate fluctuations were normal, the time was recorded and the vehicle was started. The starting point of the test was a distance before the hairpin curve, in order to stabilize the driver's condition. The driver performs natural driving (Hu 2019). After passing the test curve, the original road returns to the starting point of the test and then stops, stops recording and saves the heart rate data, and the tester records the stop time of various instruments. The test procedure is shown in Figure 3.

1.4. Processing method of test data

Figure 4 shows the overall heart rate collection range. The *red* part is the heart rate collection range of the curve segment (easement curve and circular curve). In order to ensure the continuity of the heart rate collection, the interval point i is the range of the heart rate taken before and after the curve is entered.

According to the output frequency of the Prince 180D rapid electrocardiograph, the original heart rate values were extracted one by one with a time interval of 5 s. According to the size of the curve angle, the hairpin curve was divided into 3 types: 1st one is the *curve angle* > 180°

(as shown in Figure 4, named curve 1, 6, 9, and 11); 2nd one is the curve angle ≈ 180° (as shown in Figure 4, named curve 2, 3, and 10); 3rd one is the 150° < *curve angle* < 180° (as shown in Figure 4, named curve 4, 5, 7, and 8). Data was collected at each curve. The heart rate data of 20 drivers who conducted natural driving tests were collected, and finally the specific data of 7 drivers were extracted for processing. Figure 5 shows the overall heart rate fluctuation of the driver D3 uphill. The same process was performed on each driver, and the heart rate value of driving under each curve was extracted.

2. Results

2.1. The overall change characteristics of heart rate

Taking the curve angle as the classification point, the heart rate fluctuation curves under the same curve were summarized, and then the overall change characteristics of the driver's heart rate were observed. The time-heart rate curves of all drivers at the same type of curve are shown in Figures 6 and 7.

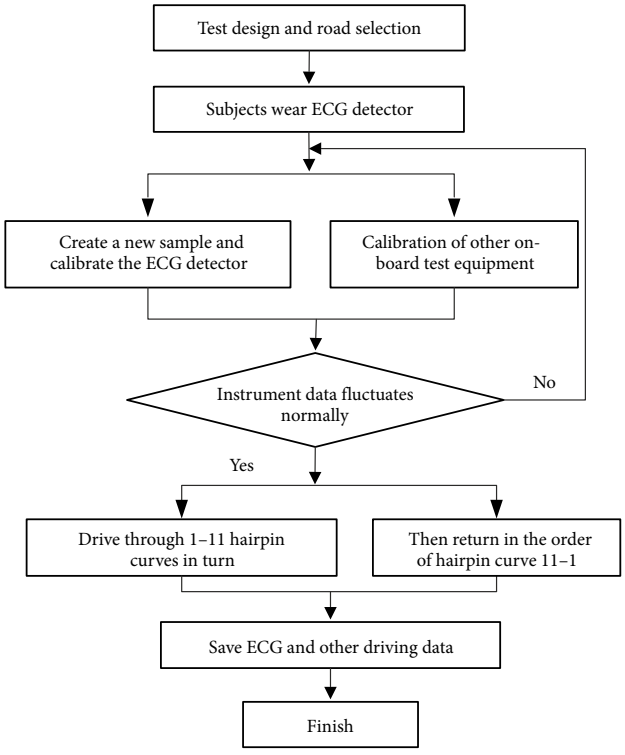

Figure 3. Test procedure

Due to individual differences and different adaptability to the driving environment, there were differences in the driver's heart rate fluctuation amplitude and the interval of the heart rate value. However, as a whole, it can be classified into 2 types: the 1st is that the heart rate value is stable at a higher level; the 2nd category is fluctuations within a lower level. The higher heart rate in the heart rate fluctuation chart was driver D5. At around 115 time/min, the maximum and minimum difference in the uphill were 7 time/min, appearing on the curve, which 150° < *curve angle* < 180°, and the difference in the downhill were 7 time/min, appears in the curve, which *curve angle* ≈ 180°, because D5 is a male, and has been driving for 10 years, but driving was only a means of transportation for daily commuting, so driving at the complex linear hairpin curve has been in a relatively tight state. The lower level fluctuation value is in the range of 65 to 95 time/min, and the maximum fluctuation value was 51 time/min in the uphill direction, which appears in the driver D1 at the curve, which *curve angle* ≈ 180°. 42 time/min downhill was the D1 driver at the curve, which 150° < *curve angle* < 180°.

Table 2 shows the mean values of the 2 types of heart rate fluctuations and their difference ratios under different curve angles of the hairpin curve: 1st type of heart rate shows that the uphill was greater than the downhill, the mean maximum heart rate was 115 bpm, which appears on the curve, which *curve angle* ≈ 180°, while the 2nd type of heart rate shows the opposite trend, the downhill was greater than the uphill, the mean maximum heart rate of 87 bpm also appears at the curve, which *curve angle* ≈ 180°. That is, although the driver's heart rate distribution range was quite different, when the *curve angle* ≈ 180°, the mean value of heart rate will reach a higher level. From the growth rate of the mean value of the 1st type of heart rate relative to the mean value of the 2nd type, it can be seen that the difference in the mean value of the 2 types

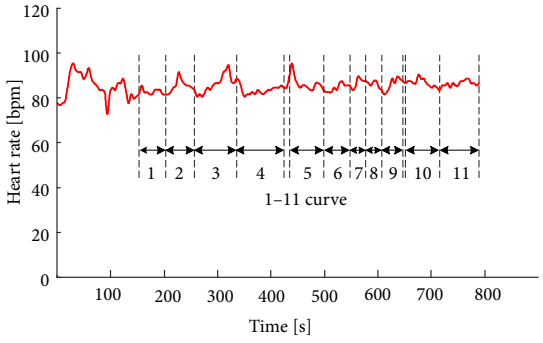

Figure 5. Overall heart rate fluctuation and curve position

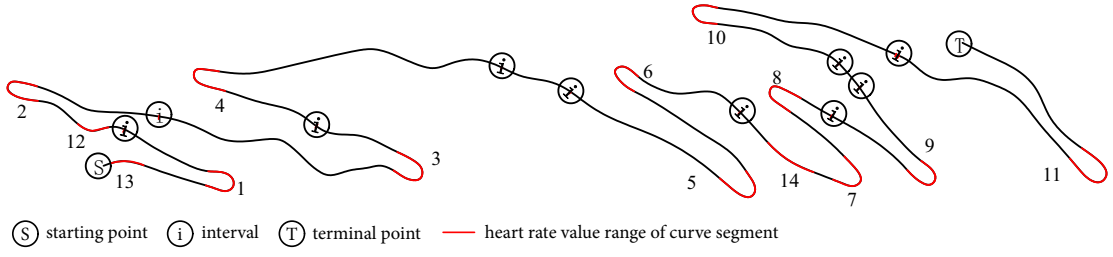

Figure 4. Schematic diagram of the location of heart rate collection

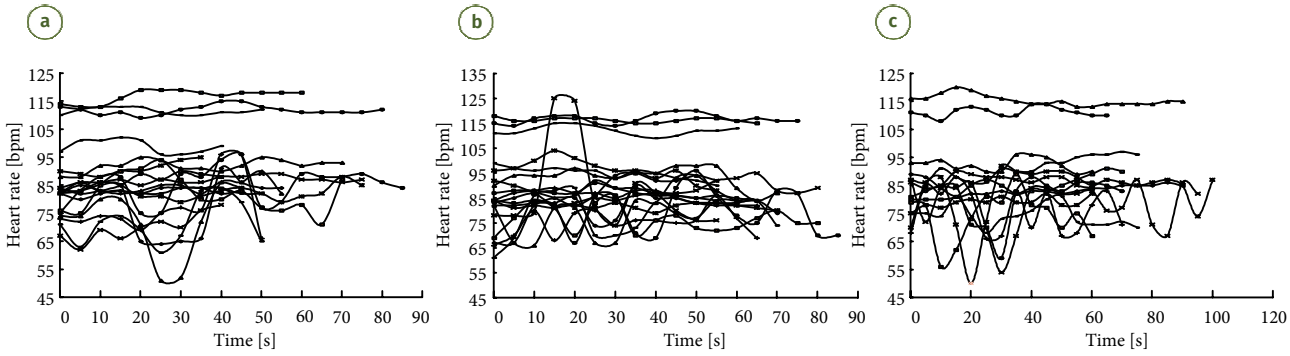

Figure 6. Distribution curve of uphill heart rate changes:
(a) *curve angle* > 180°; (b) *curve angle* ≈ 180°; (c) 150° < *curve angle* < 180°

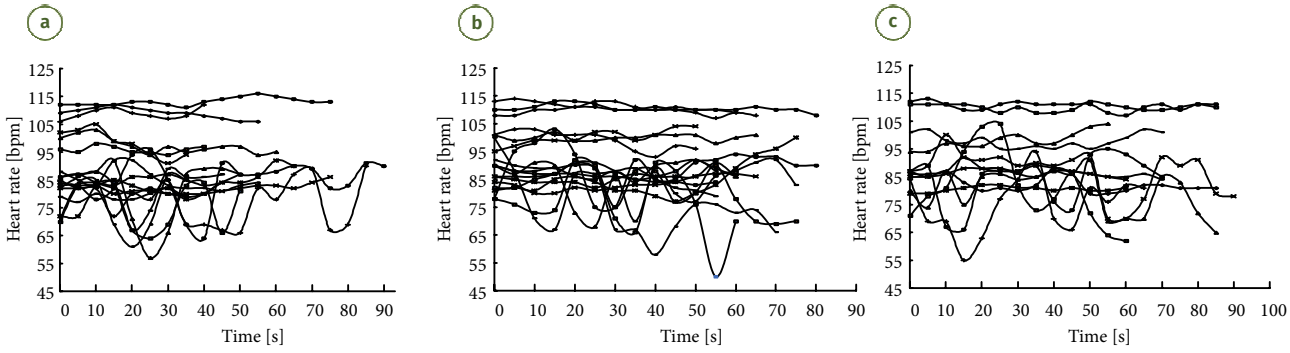

Figure 7. Distribution curve of downhill heart rate changes:
(a) *curve angle* > 180°; (b) *curve angle* ≈ 180°; (c) 150° < *curve angle* < 180°

Table 2. Mean and variation of heart rate under different curve angles

	curve angle > 180°		*curve angle* ≈ 180°		150° < *curve angle* < 180°	
	uphill	downhill	uphill	downhill	uphill	downhill
1st-type mean [bpm]	113.3415	110.7297	115.2093	110.4545	113.6061	110.1944
2nd-type mean [bpm]	83.58553	85.71614	85.15657	86.64071	82.5496	85.70253
Mean growth rate [%]	35.59939	29.18189	35.29115	27.48574	37.62157	28.57783

of heart rate was more significant when going uphill, the highest was 37.6%, which appears at the curve, which angle is less than 180°, and the maximum in the downhill was 29.18%, which appears on the curve, which angle is more than 180°. On the whole, the mean value of heart rate at the curve, which *curve angle* ≈ 180° was the largest, but the fluctuation range was smaller compared to the other 2 type of curves.

The heart rate fluctuation trends of different drivers at the same type of curve angle and different types of curve angle of the same driver show multiple trends, indicating that the heart rate changes at the hairpin curve are not only related to the driver, but also closely related to the shape of the curve and the external environment, etc.

Therefore, by dividing the curve area, as shown in Figure 8a. The heart rate at the straight segment before entering the curve (defined as in to the curve), the curve segment composed of the transition curve and the circular curve (defined as middle of the curve), and the straight segment exiting the curve (defined as out of the curve) were classified. The extracted heart rate value area is shown in Figure 8b, which shows the heart rate fluctuation value of the driver D1 in the uphill direction of curve 2 (position of the curve is shown in Figure 4). In order to further study the characteristics of heart rate changes in different areas of the curve.

After summarizing, as shown in Figure 9. From the overall heart rate distribution and growth trend, the driver's heart rate in the middle of the curve was lower than other 2 parts, which was different from the general driver's perception of tight cornering. In this way, the characteristics of the driver's heart rate load index change and the change characteristics of each mode were explored.

2.2. Overall HRI characteristics

The HRI is the growth rate of the heart rate value at a certain moment (HR_i) relative to the minimum heart rate (HR_{min}) when turning. The heart rate value and the minimum heart rate as shown in Figure 8b. It reflects the driver's heart rate fluctuation amplitude range when turning.

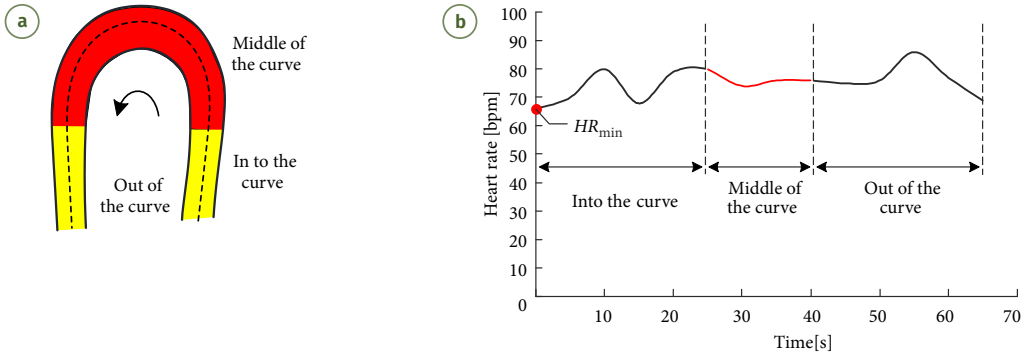

Figure 8. Schematic diagram of the division of heart rate zones at curves: (a) curve zone; (b) heart rate fluctuations in different zones

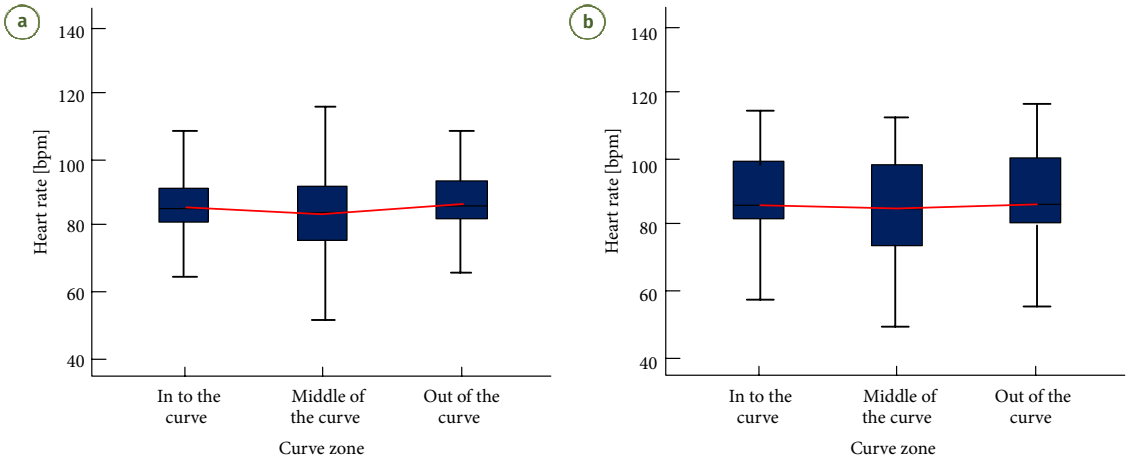

Figure 9. Heart rate distribution in different areas of the curve: (a) uphill; (b) downhill

That is, the smaller the heart rate growth rate, the smaller the influence of the outside world on the driver when turning. The specific calculation method is as follows:

$$HRI = \frac{HR_i - HR_{\min}}{HR_{\min}}, \quad (1)$$

where: HR_i is the heart rate value at time i; $HR_{\min}$ is the minimum value of the heart rate.

Calculate the heart rate of all drivers to obtain the HRI of each curve. Figure 10a shows the HRI curve of the driver D3 driving uphill on curve 2, and Figure 10b shows the heart rate growth curve of D3 in all uphill curves. Figure 11 shows the cumulative frequency of the overall HRI of the hairpin curve, and the 15th, 50th, 85th, and 95th quantiles were extracted. The overall growth trend shows that there were 2 obvious inflection points in the cumulative frequency curve, inflection point 1 was 50th, the cumulative frequency increase slope before this inflection point was large, and the HRI was generally low. Inflection point 2 was 95th, and the cumulative frequency curve after this inflection point tend to be flush. From the cumulative frequency Figure 11 of the HRI and the specific percentile Table 3, it can be seen that the maximum value and the percentile of the maximum HRI in the curve show that the uphill direction was greater than the downhill direction. However, the total average of all maximum HRI shows a phenomenon that the downhill was greater than the uphill. Indicating that the heart rate fluctuates more when downhill than uphill. For the mean value of the HRI, the maximum value still shows that the uphill was greater than the downhill, and the total mean downhill value still shows a situation that was greater than the uphill. This again verifies the large fluctuation of the driver's heart rate when going downhill, and the mean value corresponds to the percentile of the specific position, the HRI of the downhill curve has changed to a state greater than that of the uphill curve from the 85th. It can also be seen from the intensity of the cumulative frequency curve that the increase interval of the mean value was mainly distributed in the 0% to 5%, and the increase interval of the max value was mainly distributed in the 5...15%.

2.3. The overall change characteristics of HRV

HRV refers to the subtle changes in the heartbeat interval, which can better reflect the driver's workload status, so it is an effective indicator for detecting and evaluating the driver's mental load. The time domain analysis method was adopted, and the RMSSD of the differentials between adjacent *R–R* intervals was used as the analysis index. The specific calculation method is as follows:

$$RMSSD = \sqrt{\frac{1}{N-1} \cdot \sum_{i=1}^{N-1} \left(RR_{i+1} - RR_i\right)}, \quad (2)$$

where: N is the total number of R waves in the analysis time, and the time interval is 5 s.

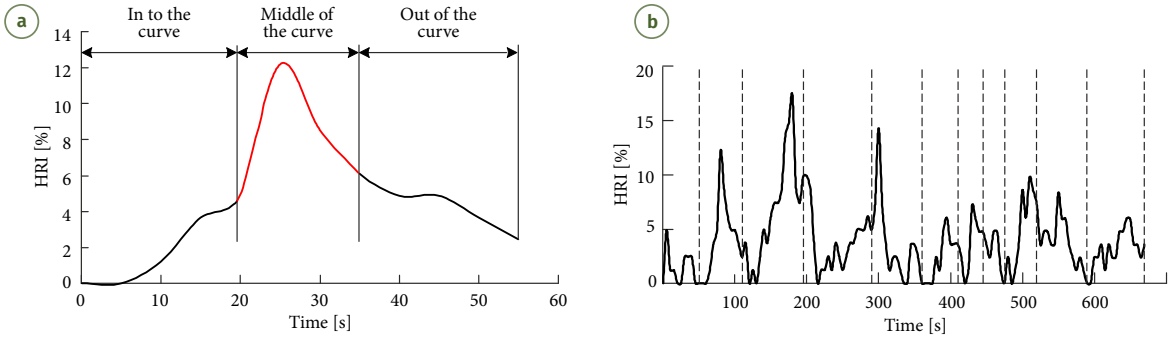

Figure 10. The curve indicates of HRI: (a) in a curve; (b) throughout the trip

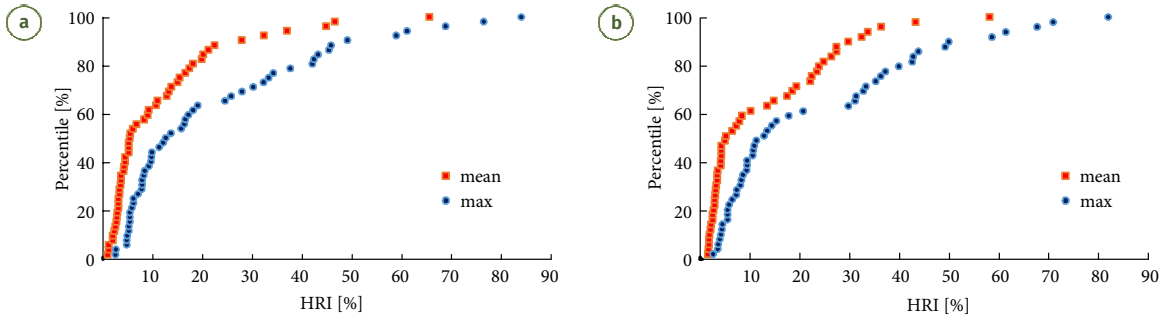

Figure 11. Cumulative frequency distribution of HRI in the uphill and downhill of the hairpin curves: (a) uphill; (b) downhill

Table 3. Statistical value and characteristic quantile value of HRI

	Max	Mean	15th	50th	85th	95th
Mean (uphill)	65.52381	11.89307	2.706630	5.611111	20.81772	40.98478
Mean (downhill)	58.15385	13.02930	2.460086	5.251442	26.97267	35.14330
Max (uphill)	84.00000	22.50786	5.407161	13.27035	44.36906	65.01502
Max (downhill)	82.00000	23.30727	5.118553	12.18971	43.39827	64.57272

Figure 12 shows the uphill heart rate variation curve of the driver D3. The max value and mean value of each curve were extracted respectively, and the mean value and max value of the heart rate variation of all drivers at the curve were accumulated in frequency. So, the overall heart rate variation characteristics of the uphill and downhill of the hairpin curves were obtained.

Figure 13 is the RMSSD mean value and max value cumulative frequency curve, and the 15th, 50th, 85th, and 95th quantiles were extracted. The overall cumulative frequency growth trend shows that, the uphill and downhill driving has an increase inflection point at the 60th quantile, and the previous HRV was concentrated in a small range. From the statistical value of the mean value of the anomaly index, it can be seen that except for the 85th quantiles whose mean value of uphill was greater than the downhill, the rest of the characteristic quantile values, the maximum value and the total average value all shows that downhill driving was greater than uphill driving. This was contrary to the rule of the HRI mentioned above. The mean value of the max value and the 15th quantiles

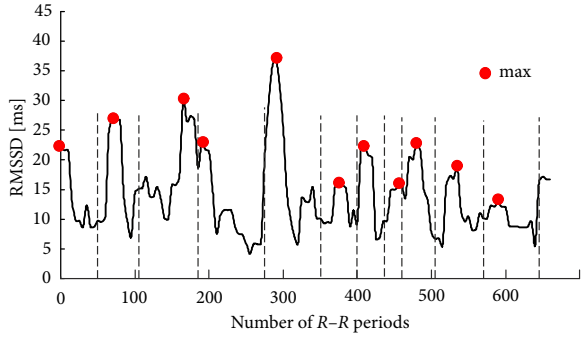

Figure 12. Extraction of the maximum value of RMSSD

shows that the downhill was greater than the uphill, and the other values shows that the uphill curve was greater than the downhill curve. That is to say, the driver's heart rate changes in adjacent sections when going uphill were generally within a relatively stable range, but there was a sudden increase or decrease in heart rate. However, during the downhill period, the overall adjacent heart rate varies greatly, but the abrupt change was small.

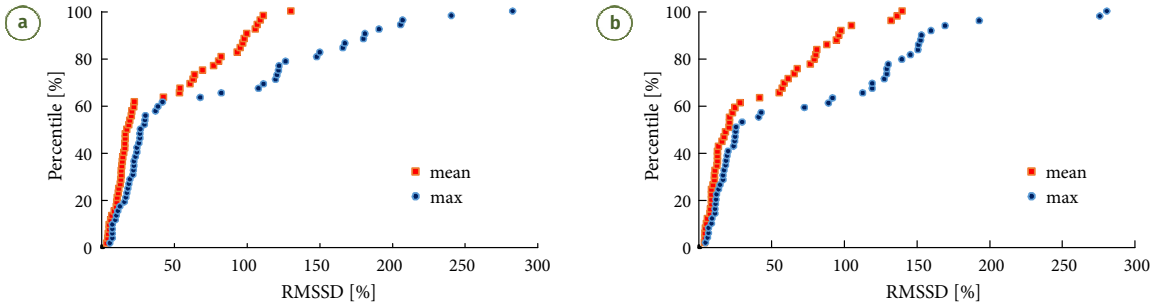

Figure 13. Cumulative frequency distribution of RMSSD in the uphill and downhill of the hairpin curves: (a) uphill; (b) downhill

Table 4. RMSSD statistical value and characteristic quantile value

	Max	Mean	15th	50th	85th	95th
Mean (uphill)	130.6223	40.99745	8.175560	17.80135	96.73591	108.6924
Mean (downhill)	140.3371	41.11662	8.265253	19.98862	85.06556	118.9857
Max (uphill)	282.7939	72.53811	11.12101	26.97336	166.9044	206.4355
Max (downhill)	280.9342	73.54912	11.5226	25.90776	151.0547	181.4141

2.4. The relationship between HRV and curve angle

The heart rate collection at individual curves is interrupted due to vibration or the driver's own motion amplitude during driving. Therefore, in order to unify the base number, take different curve angle as classification points to discuss the frequency difference characteristics of the total number of distribution intervals under different curve angles. It can be seen from the Figure 14 that the distribution interval of the RMSSD mean value was mainly concentrated in 0...30 ms. The mean value of the heart rate variability under each curve angle of the uphill was the highest in the range of 10...20 ms, and the curve, which *curve angle* > 180°; curve which *curve angle* ≈ 180°; curve, which 150° < *curve angle* < 180°. While the three intervals of 0...30 ms were more evenly distributed in the downhill, the variation of the curve, which *curve angle* > 180° was mainly concentrated in the range of 10...20 ms, and the other 2 types of curves were mainly concentrated in the 0...10 ms. On the whole, it can be seen that the average value of the HRV at the curve, which *curve angle* > 180° was smaller than the HRV under the other two types of curves.

In Figure 15, for the distribution and proportion of the HRV max value, it can be seen that there was an obvious regional concentration distribution in the uphill and downhill. The 1st type interval was 0...30 ms, when the HRV max value was lower, and the 2nd type interval was ≈100 ms when the HRV max value was higher. It can be seen from the proportions of the different curve angles in each interval that the curve, which 150° < *curve angle* < 180° has a significant increase in the proportion of the curve. The max value of the uphill was concentrated in 20...30 ms, and the max value of the downhill was concentrated in 10...20 ms. The max proportions of the 2 types of HRV intervals shows a phenomenon that the downhill curve was larger than the uphill curve in the curve, which 150° < *curve angle* < 180°, that is, the HRV values of the downhill of the curve, which 150° < *curve angle* < 180° were more concentrated in 2 areas.

3. Discussion

3.1. HRI modes of hairpin curves

The HRI is an important indicator of quantitative analysis, which can describe the driver's heart rate change amplitude compared to the whole when turning, reflecting the influence of the outside world on the driver when turning. According to the calculation of the HRI calculated in Section 2.2, the HRI of the driver in the curve segment was extracted, and the data interception range was shown in the red area in the curve as shown in Figure 10a.

Combined with the curve environment, a curve with a wide view or only sparse trees obscured was defined as a good visibility, as show in Figure 17a. A retaining wall or soil slope on one side was defined as a normal visibility, as show in Figure 17b. The presence of retaining walls or soil slopes on both sides was defined as poor visibility, as show in Figure 17c. Taking the floating trend of the HRI as an indicator, 4 modes were divided:

- ***Mode I: continuous tension***. As shown in Figure 16a. At the beginning of the curve, the heart rate gradually rises with the increase of the distance into the curve, and reaches the maximum when leaving the curve. This type of driver was most affected by the outside environment and was in a constant tension when turning. Mainly concentrated in the uphill of curve 5 (Figure 4) and downhill curves in curves 5 and 7, from the view distance and the environment, the inner side of the uphill and downhill of curve 5 was a retaining wall. The inner side of the downhill of curve 7 was a soil slope, and the outer side has a retaining wall, so the overall visibility was poor;

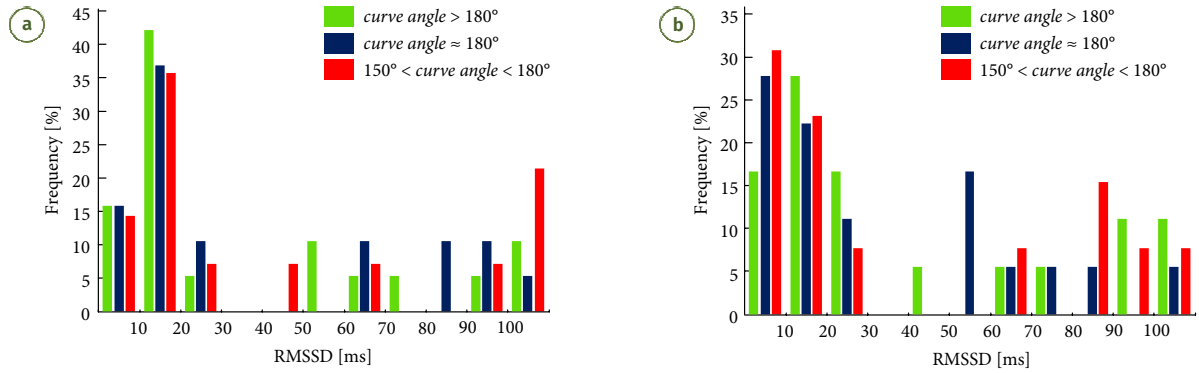

Figure 14. The frequency distribution of the RMSSD mean value at different curve angles: (a) uphill; (b) downhill

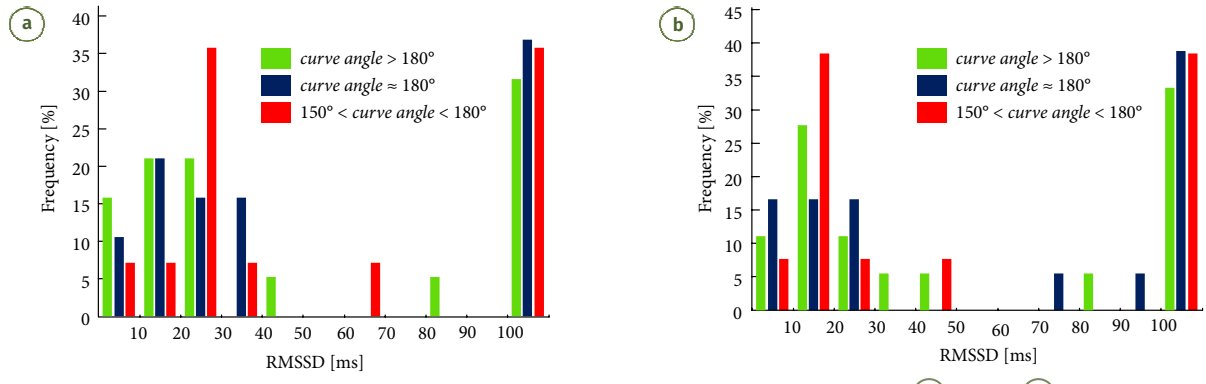

Figure 15. The frequency distribution of the RMSSD max value at different curve angles: (a) uphill; (b) downhill

- ***Mode II: relax gradually***. As shown in Figure 16b. The unknown state before entering the curve makes the driver's heart rate value reach the highest value. As the distance into the curve increases, after the driver makes a reasonable prediction of the external environment, his heart rate was reduced until he leaves the curve. It is mainly concentrated on the uphill of curve 10 and the downhill of curves 2, 4 and 9. When driving in the downhill of curve 2, there was a soil slope on the inner side, and there was a small amount of vegetation on the inner side of the downhill of curve 4 and curve 9. So, the visual communication performance was average. And there was vegetation on the inner side of curve 10, but it was sparse, so the overall visibility was better;
- ***Mode III: relaxation–tension***. As shown in Figure 16c. From the fluctuating trend of the HRI, it can be seen that there was a valley in the middle, the driver's heart rate gradually decreases as the distance into the curve increases, and the mentality gradually stabilizes to the curve, and then, the heart rate gradually rises when exiting the curve. In other words, the heart rate of this type of driver will drop when the external influence is large, and the mentality will be more stable. Mostly concentrated on the uphill direction of the curve, mainly at curve 1 and curve 4. The inner side of the curve 1 has a relatively low soil slope, and the inner side of the curve 4 was sheltered by sparse vegetation, and the overall visibility was better. A small amount exists in the downhill direction of the curve 9, and the visual communication performance was average;
- ***Mode IV: tension–relaxation***. As shown in Figure 16d. When entering a curve, the heart rate was in a state of increasing, and reaches a max point when turning. As the driver leaves the curve, the heart rate gradually decreases. The heart rate changes of such drivers conform to the state of "the more nervous the heart rate changes". Mostly concentrated on downhill curves, with curve 10 as the main one, with retaining walls on the inner side, and general visibility.

3.2. Comparison and verification of general curves

Take 3 general curves at the same time, the radius of the curve is 35 m (Figure 4, curve 12), 80 m (Figure 4, curve 13), and 120 m (Figure 4, curve 14), and the road parameters are shown in Table 5. Calculating the HRI in the curve, 4 types of HRI modes were also obtained, as shown in Figure 18, and the proportions of patterns I to IV were 7:6:5:2. Compared with the ratio of 18.3:25.2:30.5:26.0 in the hairpin curve HRI mode, the HRI at the general curve was mainly concentrated in 2 types of modes: straight up and straight down. Among them, the general curve with a radius of 120 m was dominated by mode II when it goes downhill. Its geographical position is at the hairpin curve 7 after going downhill and out of the curve. Since the HRI mode at curve 7 downhill was dominated by Mode I, the heart rate was at a relatively high level when exiting the curve, and the driver's heart rate gradually decreases after leaving the curve 7 and entering a normal curve, which further confirms the difference in heart rate between a large radius curve and a hairpin curve.

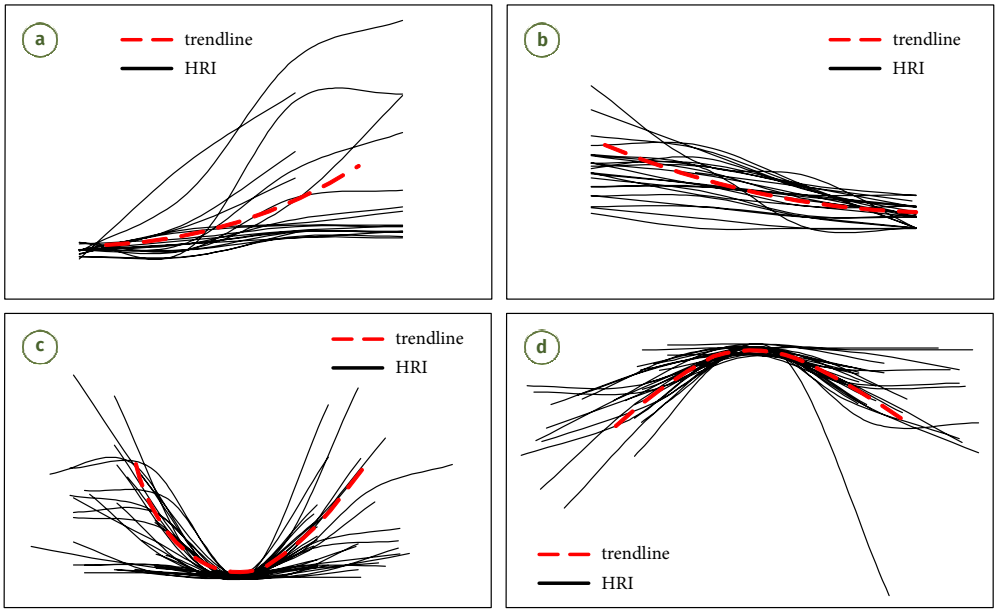

Figure 16. HRI modes of hairpin curves: (a) Mode I; (b) Mode II; (c) Mode III; (d) Mode IV

Figure 17. The roadside environment of the hairpin curves:
(a) good conditions on the roadside; (b) general roadside conditions; (c) poor roadside environment

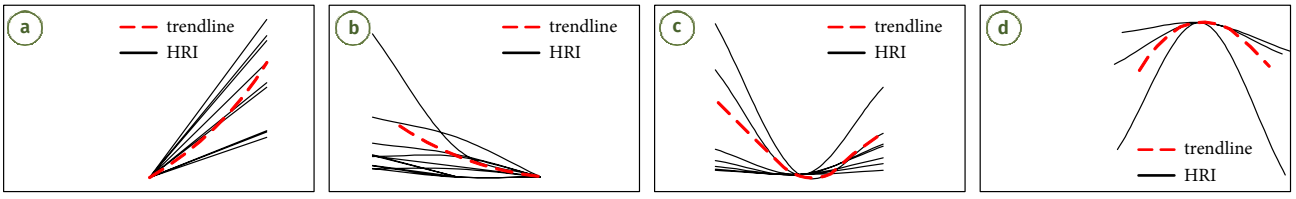

Figure 18. HRI modes of general curves: (a) Mode I; (b) Mode II; (c) Mode III; (d) Mode IV

Table 5. Geometric parameters of the general curves

Number	Radius [m]	Curve angle [°]	Curve length [m]	Easing curve length [m]	Slope [%]	Pre-curve/post-curve slop [%]	Lane width [m]
1	35	64.40	64.51	25	2	2/7	3.25,3.25
2	80	37.12	76.95	25	8.4	8.4/8.4	3.25,3.25
3	120	29.2	86.46	25	9	3.5/9	3.25,3.25

Conclusions

At the hairpin curve, the overall heart rate distribution range of passenger car drivers presents 2 trends, the one is the heart rate value is higher and stable, the other is fluctuates within a lower level. Taking the *curve angle* as the classification point, the mean heart rate values were higher when the curve angle ≈ 180°, with a maximum of 115 bpm for 1st type and 87 bpm for 2nd type. The range of heart rate fluctuations was more concentrated at the *curve angle* of 180° than at the other 2 angles of the curve. The growth rate of the mean heart rate values in both types was greater uphill than downhill.

By dividing the curve into 3 areas: in to the curve, in the middle of the curve, and out of the curve, the overall fluctuation range of the heart rate in the middle of curve was at the lowest level. That is, as the distance into the curve increases, the difference between the heart rate values of different drivers at the curve section reaches the minimum, and it rises further when exiting the curve.

Cumulative frequency distribution curves for the HRI in both the uphill and downhill directions for drivers driving in hairpin curve have 2 inflection points, 50th and 95th, respectively, reflecting the concentration of HRI for the majority of drivers. The growth interval of the mean HRI was mainly distributed in 0…5%, while the increase interval of max value was mainly distributed in 5…15%. The fluctuation of the heart rate when going downhill was more significant than when going uphill, that is, the driver was more susceptible to the influence of the external environment when going downhill.

There is an inflection point in the RMSSD cumulative frequency curve in the uphill and downhill directions, at 60th, reflecting the concentration of HRV characteristics for the majority of drivers. When going uphill, the driver's heart rate changes in the adjacent section were generally within a relatively stable range, but there was a sudden increase or decrease in the heart rate, while the overall change in the adjacent heart rate during the downhill period was relatively large, but abruptly small. The mean RMSSD is smallest when the *curve angle* > 180° and is concentrated in the range of 10…20 ms.

The HRI trend at the hairpin curve can be divided into 4 modes: "continuous tension", "relax gradually", "relaxation–tension", and "tension–relaxation". Heart rate fluctuation patterns are closely related to the curve environment and visual distance, that is, the more complicated the curve environment and the worse the viewing distance condition, the more significant the fluctuation of the driver's heart rate will be.

The ratio of modes I to IV at the general curves was 7:6:5:2 and 18.3:25.2:30.5:26.0 at the hairpin curves, i.e., the hairpin curves were more concentrated in modes with greater heart rate volatility (Modes III and IV) than the general curves HRI trends, while the general curves were concentrated in more single change trends (Modes I and II).

This article mainly discusses the characteristics of daytime-heart rate changes of drivers of passenger cars, and will further study the characteristics of heart rate changes of drivers of different models and different driving periods in the follow-up.

Funding

This research was supported by the:

- National Key R&D Program of China (Grant No 2018YFB1600500);
- Science and Technology Research Project of China Railway Siyuan Survey and Design Group Co. Ltd. (Grant No 2019K091-1);
- National Natural Science Foundation of China (Grant No 52072291).

Author contributions

Ying Chen participated in experimental design, data collection and analysis, article writing and article revision.

Xiaohui Wang and *Xiaobo Zhang* were responsible for experimental funding support and experimental ideas.

Haiyuan Chen participate in data collection.

Zhigang Du participate in experimental ideas.

Jin Xu participate in the idea of experimentation and modify the article.

Disclosure statement

Authors declare that they have no conflicts of interest.

References

Eboli, L.; Guido, G.; Mazzulla, G.; Pungillo, G. 2017. Experimental relationships between operating speeds of successive road design elements in two-lane rural highways, *Transport* 32(2): 138–145. https://doi.org/10.3846/16484142.2015.1110831

Feng, D.; Chen, F.; Pan, X. 2017. Research on driver physiological load at the lowest point of city river-crossing tunnels, *Transportation Research Procedia* 25: 1494–1502. https://doi.org/10.1016/j.trpro.2017.05.178

Feng, Z.; Yang, M.; Zhang, W.; Du, Y.; Bai, H. 2018. Effect of longitudinal slope of urban underpass tunnels on drivers' heart rate and speed: a study based on a real vehicle experiment, *Tunnelling and Underground Space Technology* 81: 525–533. https://doi.org/10.1016/j.tust.2018.08.032

Gromer, M.; Salb, D.; Walzer, T.; Martínez Madrid, N.; Seepold, R. 2019. ECG sensor for detection of driver's drowsiness, *Procedia Computer Science* 159: 1938–1946. https://doi.org/10.1016/j.procs.2019.09.366

Hu, J. 2019. *Research on the Psychological Load of Mountain City Interchange Based on Natural Driving*. Chong Qing Jiaotong University, Chong Qing, China. (in Chinese).

Li, H.; Zhu, S.; Qi, C.; Yang, F.; Gao, M. 2015. Driver's psychological and physiological reaction analysis on snow-covered road in North Forest region, *Journal of Northeast Forestry University* (5): 118–122. https://doi.org/10.13759/j.cnki.dlxb.20150522.006 (in Chinese).

Miller, E. E.; Boyle, L. N. 2015. Driver behavior in road tunnels: association with driver stress and performance, *Transportation Research Record: Journal of the Transportation Research Board* 2518: 60–67. https://doi.org/10.3141/2518-08

Patel, M.; Lal, S. K. L.; Kavanagh, D.; Rossiter, P. 2011. Applying neural network analysis on heart rate variability data to assess driver fatigue, *Expert Systems with Applications* 38(6): 7235–7242. https://doi.org/10.1016/j.eswa.2010.12.028

Peng, Z.; Rong, J.; Wu, Y.; Zhou, C.; Yuan, Y.; Shao, X. 2021. Exploring the different patterns for generation process of driving fatigue based on individual driving behavior parameters, *Transportation Research Record: Journal of the Transportation Research Board* 2675(8): 408–421. https://doi.org/10.1177/0361198121998351

Qiao, J.; Li, S.; Liu, W. L.; Liu, W. Y. 2020. Relationship between driver's heart rate change and curved slope ratio of rebuilt

and expanded roads and driving speed difference, *Journal of Fuzhou University* (*Natural Science Edition*) 48(1): 105–109. (in Chinese).

Qin, P.; Wang, M.; Chen, Z.; Yan, G.; Yan, T.; Han, C.; Bao, Y.; Wang, X. 2021. Characteristics of driver fatigue and fatigue-relieving effect of special light belt in extra-long highway tunnel: a real-road driving study, *Tunnelling and Underground Space Technology* 114: 103990. https://doi.org/10.1016/J.TUST.2021.103990

Russo, F.; Biancardo, S. A.; Busiello, M. 2016. Operating speed as a key factor in studying the driver behaviour in a rural context, *Transport* 31(2): 260–270. https://doi.org/10.3846/16484142.2016.1193054

Sang, Y.; Li, J. 2012. Research on Beijing bus driver psychology fatigue evaluation, *Procedia Engineering* 43: 443–448. https://doi.org/10.1016/j.proeng.2012.08.076

Wadhwa, A.; Roy, S. S. 2020. Driver drowsiness detection using heart rate and behavior methods: a study, in K. C. Lee, S. S. Roy, P. Samui, V. Kumar (Eds.). *Data Analytics in Biomedical Engineering and Healthcare*, 163–177. https://doi.org/10.1016/B978-0-12-819314-3.00011-2

Wang, J. Z.; Alli, S. 2020. Safety risk assessment of plateau highway corner value based on driver's physiological load, *Science Technology and Engineering* (7): 2939–2943. (in Chinese).

Wolkow, A. P.; Rajaratnam, S. M. W.; Wilkinson, V.; Shee, D.; Baker, A.; Lillington, T.; Roest, P.; Marx, B.; Chew, C.; Tucker, A.; Haque, S.; Schaefer, A.; Howard, M. E. 2020. The impact of heart rate-based drowsiness monitoring on adverse driving events in heavy vehicle drivers under naturalistic conditions, *Sleep Health* 6(3): 366–373. https://doi.org/10.1016/j.sleh.2020.03.005

Wu, Y.; Zhao, X.; Rong, J.; Ma, J. 2013. Effects of chevron alignment signs on driver eye movements, driving performance, and stress, *Transportation Research Record: Journal of the Transportation Research Board* 2365: 10–16. https://doi.org/10.3141/2365-02

Xiao, D. Q.; Shen, Z. W.; Xu, X.C. 2017. Investigating the impact of greenery on the driver's psychology at a freeway tunnel portal, in *Civil, Architecture and Environmental Engineering: Proceedings of the International Conference ICCAE*, 4–6 November 2016, Taipei, Taiwan, 1: 159–166. https://doi.org/10.1201/9781315226187-27

Xu, J.; Liu, X.-M.; Hu, J. 2020. Analysis of driver mental load on helical ramps and helical bridges based on naturalistic driving data, *Journal of Transportation Systems Engineering and Information Technology* (3): 212–218. https://doi.org/10.16097/j.cnki.1009-6744.2020.03.032 (in Chinese).

Zeng, C.; Wang, W.; Chen, C.; Zhang, C.; Cheng, B. 2020. Sex differences in time-domain and frequency-domain heart rate variability measures of fatigued drivers, *International Journal of Environmental Research and Public Health* 17(22): 8499. https://doi.org/10.3390/ijerph17228499

Zhang, J.; Liu, H.; Chen, J.; Tian, Z.; Wang, Z. 2015. On the relationship between the drivers' heart-beating rate and the curve radius of long and steep slop, *Journal of Safety and Environment* (4): 140–143. (in Chinese).

Zhao, L.; Zhang, M. L. 2012. Influence of radius of horizontal curve on driver's psychology and physiology on the two-lane mountain highway, *Applied Mechanics and Materials* 226–228: 2335–2339. https://doi.org/10.4028/www.scientific.net/AMM.226-228.2335

Zhao, T.; Qi, C.; Zhu, S.; Gao, M.; Wang, Y. 2016. Study on influence of complexity of highway alignment on driver's HRV, *China Safety Science Journal* (2): 6–12. https://doi.org/10.16265/j.cnki.issn1003-3033.2016.02.002 (in Chinese).

Zhu, R. 2020. A review of research on driving fatigue detection based on physiological signals, *Chinese Journal of Ergonomics* 26(4): 82–86. (in Chinese).